ANOMALOUS TRANSPORT IN TOKAMAKS WITH OHMIC AND AUXILIARY HEATING

G. Becker

IPP III/109

March 1986

MAX-PLANCK-INSTITUT FÜR PLASMAPHYSIK

8046 GARCHING BEI MÜNCHEN

MAX-PLANCK-INSTITUT FÜR PLASMAPHYSIK

GARCHING BEI MÜNCHEN

ANOMALOUS TRANSPORT IN TOKAMAKS WITH OHMIC AND AUXILIARY HEATING

G. Becker

IPP III/109 March 1986

Die nachstehende Arbeit wurde im Rahmen des Vertrages zwischen dem Max-Planck-Institut für Plasmaphysik und der Europäischen Atomgemeinschaft über die Zusammenarbeit auf dem Gebiete der Plasmaphysik durchgeführt.

IPP III/109 G. Becker

ANOMALOUS TRANSPORT IN TOKAMAKS WITH OHMIC AND AUXILIARY HEATING

March 1986

Abstract. The anomalous electron heat diffusivity χ_e is investigated by a power scan of the injection heating and by the time evolution of L (low confinement) discharges. It is shown that deviations from the ohmic scaling occur if the non-ohmic electron heating locally exceeds the ohmic power density. The change in scaling is attributed to a self-regulating process connected with strong turbulence, which adjusts χ_e to the injection heating with its different dependence on the plasma parameters. With this process, the shape of the electron temperature profile is not constrained by the profile consistency. It is further concluded that the different scalings are not due to other instabilities or saturation effects, which is consistent with the expected highly turbulent state. Constraints on χ_e are derived from the electron and ion energy equations and the shape of the measured electron temperature profiles. For small injection power complex χ_e scalings result which cannot be represented by superposing the ohmic and L scalings.

1. Introduction

The anomalous cross-field electron heat conduction and diffusion observed in tokamaks with ohmic and auxiliary heating are ascribed to turbulent field fluctuations (strong turbulence) driven by instabilities. As reliable microinstability-based diffusivities are not available at present, empirical scalings determined by means of transport modelling of many series of discharges are preferred. Results from simulations of neutral-beam-heated L (low) and H (high confinement) discharges in ASDEX have been reported in Refs. 1-3. The flux-surface-averaged electron heat diffusivity χ_e and the diffusion coefficient D exhibit a scaling in injection-heated plasmas which largely differs from that with ohmic heating /1-4/. It was demonstrated that the ohmic transport scaling is not a universal plasma quality which is

independent of the heating method.

One possible explanation for the different scaling is that neutral injection changes the transport mechanism, i.e. the underlying instabilities and/or saturation effects. There might exist a threshold parameter which distinguishes between the confinement regimes. Another possibility is that the transport mechanism itself remains unchanged. Rather self-regulating processes connected with strong turbulence modify the χ_e scaling, so that it adjusts to the injection heating with its different variation with the plasma parameters. These questions will be pursued by studying the transition between ohmic and L confinement.

This report deals with the anomalous transport in the ohmic, L and intermediate regimes. Results from transport computations (with the BALDUR code /5,6/) are used. The transition between the regimes can be explored by following the time evolution of L discharges and by scanning the injection power.

Section 2 presents the constraints on χ_e resulting from the steady-state electron energy balance and experimentally observed profile shapes of the electron temperature in ohmically and injection-heated plasmas. Then, in Section 3, the transition between ohmic and L transport is investigated by a power scan of the injection heating and interpreted in terms of the ratio of the locally absorbed beam power density and ohmic power density. Section 4 deals with the influence of the ion-electron energy tansfer rate on confinement during the L phase after the injection period. Finally, in Section 5, the consequences of the χ_e constraints for the empirical scaling relations are discussed.

2. Constraints on χ_e with ohmic and injection heating

The steady-state electron energy equation and measured T_e profile shapes are used to derive constraints for the electron heat diffusivity.

In the stationary ohmic and neutral-beam-heated phases of ASDEX characteristic shapes of $T_e(r)$ are observed. This is illustrated by Fig. 1, which shows an example of the time evolution of the electron temperature profile in an L discharge with an injection period of 400 ms ($\bar{n} = 2.4 \times 10^{13}$ cm^{-3},

I_p = 280 kA and absorbed total beam power P_{abs} = 2.0 MW). The time-resolved T_e profiles are measured by multi-pulse Thomson scattering (every 4 cm) and transformed to concentric circular flux surfaces. As can be seen, a Gaussian shape is found during the stationary ohmic phase. After the beginning of neutral injection (t_{on} = 1.12 s), the T_e profile changes to an approximately triangular shape which is then maintained during the whole injection period. The 'confinement zone' (shaded in Fig. 1) is defined by $r_{q=1} < r < 0.9\,a$, where a is the plasma radius equal to the separatrix radius of 40 cm.

The steady-state electron and ion energy equations with ohmic heating approximately read

$$-\mathrm{div}\,\vec{q}_e + \eta j_t^2 - P_{ei} = 0, \qquad (1)$$

$$-\mathrm{div}\,\vec{q}_i + P_{ei} = 0 \qquad (2)$$

Except at very high densities, the ion heat conduction and P_{ei} are negligibly small compared with the electron heat loss, yielding

$$\frac{1}{r}\frac{d}{dr}\left(r\, n\, \chi_e \frac{dT_e}{dr}\right) + \eta j_t^2 \approx 0, \qquad (3)$$

with $\eta j_t^2 = E_t j_t$ and $r j_t = c/4\pi\, d(rB_p)/dr$. Under stationary conditions the toroidal electric field E_t is radially constant. Integration then leads to

$$\chi_e^{OH}(r) = \frac{c}{4\pi} E_t \frac{B_p(r)}{n(r)\left|\frac{dT_e}{dr}\right|}. \qquad (4)$$

With the Gaussian-shaped electron temperature profiles observed,

$$T_e(r) = T_e(0)\exp\left(-\alpha \frac{r^2}{a^2}\right), \qquad (5)$$

where α is an approximate constant, one obtains the constraint /7/

$$\chi_e^{OH}(r) = \frac{c}{8\pi} \frac{a^2}{\alpha} E_t \frac{B_p(r)}{r\, n(r)\, T_e(r)}. \qquad (6)$$

It is obvious from the derivation that the dependence on $B_p(r)$ is due to the ohmic heating.

With auxiliary heating the steady-state electron and ion energy equations approximately read

$$-\text{div}\ \vec{q}_e + \eta j_t^2 + P^e_{aux} - P_{ei} = 0, \tag{7}$$

$$-\text{div}\ \vec{q}_i + P^i_{aux} + P_{ei} = 0, \tag{8}$$

where $P_{aux} = P^e_{aux} + P^i_{aux}$ is the absorbed power density of the auxiliary heating.

Neglecting again the ion heat conduction yields

$$\frac{1}{r}\frac{d}{dr}\left(rn\,\chi_e \frac{dT_e}{dr}\right) + \eta j_t^2 + P_{aux} \approx 0 \tag{9}$$

and

$$\chi_e(r) = \left[\frac{c}{4\pi}\, E_t\, B_p(r) + \frac{1}{r}\int_o^r P_{aux}(r')\, r'dr'\right] n(r)^{-1} \left|\frac{dT_e}{dr}\right|^{-1} \tag{10}$$

With $P_{aux} = 0$ the ohmic result is reproduced (see Eq. (4)). The power density of the ASDEX neutral injection system can be approximated by $P_b(r) = \alpha_b/r$ with $\alpha_b = P_{abs}/(4\pi^2 R_o a)$ and major radius R_o. Substitution in Eq. (10) yields

$$\chi_e(r) = \left(\frac{c}{4\pi} E_t\, B_p(r) + \alpha_b\right) n(r)^{-1} \left|\frac{dT_e}{dr}\right|^{-1}. \tag{11}$$

For very large injection power one obtains

$$\chi_e^L(r) = \alpha_b\, n(r)^{-1} \left|\frac{dT_e}{dr}\right|^{-1}. \tag{12}$$

A triangular electron temperature profile (see Fig. 1) given by

$$T_e(r) \simeq T_e(0)\left(1 - \frac{r}{a}\right) \tag{13}$$

yields the constraint

$$\chi_e^L(r) \simeq a\,\alpha_b\, T_e(0)^{-1}\, n(r)^{-1}. \tag{14}$$

Comparing this relation with Eq. (6) shows that the χ_e scalings depend on the heating method and its variation with the plasma parameters. Neutral injection does not introduce a $B_p(r)$ dependence in contrast to ηj_t^2. Owing to $j_t(r) \sim T_e^{3/2}(r)$ the ohmic heating and electron temperature profiles are

strongly coupled, whereas $P_b(r)$ is a function of the target density and injection energy. It is obvious that the quantities in Eqs. (3) and (9) strongly interact. Their profiles are expected to adjust self-consistently. The stationary states reached are characterized by Gaussian-shaped $T_e(r)$ and χ_e^{OH} scaling with ohmic heating, and by triangular T_e profiles and χ_e^L with neutral injection.

It is obvious from Eq. (11) that the local transport in the intermediate range cannot simply be represented by superposing the ohmic and L scalings ($\chi_e \neq \chi_e^{OH} + \chi_e^L$). The beam heating modifies the ohmic contribution by changing E_t and the T_e profile shape, i.e. by breaking up the constraint of Eq. (6). On the other hand, the ohmic heating modifies the beam-heating contribution in Eq. (11). There occur rather complex, mixed χ_e scalings which should be very difficult to determine from scans of the heating power, density and plasma current by means of transport modelling.

It is concluded that a sufficiently large auxiliary heating perturbs the adjusted ohmic state with self-consistent profiles. According to Eq. (9), marked deviations from the ohmic scaling should occur for local ratios $P_{aux}/(\eta j_t^2) \gtrsim 0.3$. This item will be checked by means of transport simulations of neutral-beam-heated discharges in Sections 3 and 4.

3. Transition between ohmic and L transport

The confinement in the intermediate range between OH and L scaling is studied by simulating a series of discharges at $\bar{n} = 2.5 \times 10^{13}$ cm^{-3}, I_p = 380 kA, $Z_{eff} = 1.5$ and $P_{OH} = 0.52$ MW with various injection powers. Figure 2 shows the increase of the electron heat diffusivity with rising absorbed beam power. Obviously, at small P_{abs} equal to 0.3 and 0.6 MW (corresponding to 1 and 2 sources) the χ_e values clearly exceed the ohmic result (cross) in the middle of the confinement zone at r = 2a/3. This explains the observed decrease of the global energy confinement time τ_E /2/. The χ_e profiles with ohmic heating and $P_{abs} = 0.6$ MW are presented in Fig. 3.

Special attention is paid to the local ratio of the injection and ohmic heating power densities. Results for various absorbed beam powers are presented in Fig. 4. It is obvious that $P_b/(\eta j_t^2) \simeq 0.3$, where the influence

of beam heating should become important, is already exceeded with P_{abs} = 0.3 MW, i.e. with one source. As shown above, the corresponding χ_e and τ_E are indeed found to deviate from the ohmic scaling. With P_{abs} = 0.6 and 0.9 MW (two and three sources), neutral injection becomes dominant in the confinement zone. This explains the observed fast transition of τ_E to the L scaling. For $P_{abs} \gtrsim 1.2$ MW the beam power density is large compared with ηj_t^2, which agrees with the essentially pure L confinement found. The same dependence of τ_E on the injection power was observed in a recent study of the intermediate confinement range /8/.

The power scan shows that the transition to the L regime correlates with the ratio $P_b/(\eta j_t^2)$ in the confinement zone. Both the deviation from the ohmic scaling and the approach to the L confinement occur at power density ratios which agree with the expected values. According to the electron energy equation, injection powers of this level perturb or break up the adjusted ohmic state. The associated change in confinement suggests that the χ_e scaling responds to the auxiliary heating by means of a self-regulating process. The fact that the coupling between the ohmic heating profile and $T_e(r)$ is broken up with neutral injection should play an important role. As the smallest injection power scarcely modifies the plasma parameters, e.g. density and temperature gradients and poloidal beta, a transition to other instabilities and/or saturation effects, i.e. to a different transport mechanism, is very unlikely.

The self-regulating or feedback process which adjusts the transport scaling to the heating method is not known. There are indications that the T_e profile shape itself is connected with the χ_e scaling by means of a strongly non-linear process. It should be mentioned that with the feedback process the shape of the electron temperature profile is not constrained. According to the 'profile consistency' model /7/, the anomalous transport in the plasma tends to maintain current profiles consistent with stability to long-wavelength MHD modes. With classical or neoclassical resistivity these profiles yield a prescription for the T_e profile shape on time scales longer than the skin time (about 100 ms with ohmic heating and up to 500 ms with neutral-beam injection). The L transport, however, appears after a time span much shorter than these skin times, so that the $T_e(r)$ shape is not constrained by the current profile.

It will be shown in Section 4 that the electron heating due to the ion-electron energy transfer has an effect similar to that of neutral injection.

4. Transport behaviour after neutral injection

A characteristic time development of the diffusivities χ_e and D in L discharges was found by means of transport simulations /1,2/. It was shown that the L phase persists for about 100 ms after the injection period. As the slowing-down time τ_s of the fast beam ions is only about 10 ms, the injection power rapidly decays. It is thus concluded that the L transport does not require the presence of injection heating, beam fuelling and direct ion heating. Simulations of many L discharges revealed that the phase with $T_i/T_e > 1$ in the central plasma, i.e. $P_{ie} > 0$, also lasts for a time span of about 100 ms. This suggests that the L phase is maintained by non-ohmic electron heating owing to the ion-electron energy transfer.

For the L discharge of Fig. 1 the time development of the electron temperature profiles measured after the end of the injection period (t_{off} = 1.52 s) is shown in Fig. 5. Although the beam-heating power is negligibly small (τ_s = 11 ms), the Gaussian-shaped T_e profiles typical of the ohmic phase are only reached after about 80 ms. The central steepening of the profiles results from the electron heating due to P_{ie}, which is largest in the plasma centre.

Profiles of $P_{ie}/(\eta j_t^2)$ after neutral injection (t_{off} = 1.31 s, τ_s = 11 ms), which were determined from simulating the L discharge with P_{abs} = 2.1 MW in Figs. 2 and 4, are presented in Fig. 6. The absorbed beam power is negligibly small at $t-t_{off}$ = 43 ms, so that the only non-ohmic heating is due to the ion-electron energy transfer. Obviously, a transport scaling different from the ohmic one should persist owing to P_{ie} in a considerable fraction of the plasma cross-section. Close to the end of the L phase ($t-t_{off}$ = 92 ms), however, the ratio of the power densities has become so small that an almost purely ohmic scaling results.

It is concluded that non-ohmic electron heating power densities (due to neutral injection or ion-electron energy transfer) which are not negligibly

small compared with ηj_t^2 lead to the L transport or to transport in the intermediate range between OH and L.

5. χ_e constraints and empirical scaling relations

In this section, the constraints for the electron heat diffusivity in ohmically and injection-heated plasmas are compared with empirical scaling relations.

Substituting $B_p/r = B_t/(q\ R_o)$ in Eq. (6) yields

$$\chi_e^{OH}(r) = \frac{c}{8\pi}\frac{a^2}{\alpha\ R_o} E_t\ B_t\ n(r)^{-1}\ T_e(r)^{-1}\ q(r)^{-1}. \qquad (15)$$

The empirical scaling relation for ohmically heated ASDEX discharges at B_t = 22 kG reads /3/

$$\chi_e^{OH}(r) = (1.9 - 2.5) \times 10^{17}\ \ n(r)^{-1}\ T_e(r)^{-1}\ q(r)^{-1}\ cm^2 \cdot s^{-1}, \qquad (16)$$

where n is in cm^{-3} and T_e is in keV.

Equation (15) shows that the radial dependence of χ_e^{OH} is determined by the profiles of n, T_e and q. Obviously, the inverse scaling with these parameters agrees with the empirical relation. Note that Eq. (15) results from ohmic heating and from using the experimental T_e profile shape, i.e. without making specific assumptions on the transport mechanism such as the underlying instabilities. As the ohmic scaling relation of Coppi and Mazzucato /9/ was also derived for Gaussian-shaped T_e profiles, its agreement with the variation of the empirical coefficient as n^{-1}, T_e^{-1} and B_t/q cannot support the assumptions on the transport mechanism, e.g. the role of the 'reconnecting modes'. The transport model rather has to be checked by its predictions for the scaling of the radially constant factors such as E_t.

For large injection power and $P_b = \alpha_b/r$ an electron thermal conductivity

$$\kappa_e^L = n(r)\ \chi_e^L(r) \simeq a\ \alpha_b\ T_e(0)^{-1} \qquad (17)$$

which is approximately constant with radius is obtained from Eq. (14).

The outstanding features of the empirical L scaling /3/

$$\chi_e^L(r) = 2.3 \times 10^4 \; r_n(r)^{-1/2} \; T_i(r)^{1/2} \; rB_p(r)^{-1} \; cm^2 \cdot s^{-1} \qquad (18)$$

are the lack of an explicit density dependence and the inverse B_p scaling. Here, $r_n = -n/(\partial n/\partial r)$ is in cm, T_i is in keV and B_p is in kG. Comparing with Eq. (14) shows that $T_e(0)$ should introduce an $n(0)$, so that $\chi_e^L \sim n(0)/n(r)$ becomes density-independent. Its radial variation, however, is given by the shape of the density profile. A scaling as $T_e(0) \sim \alpha_b/n(0)$ is consistent with the expected increase of the central electron temperature with the absorbed beam power per particle.

6. Conclusions

The anomalous transport in the ohmic, L and intermediate regimes was investigated by means of a scan of the injection power and the time development of L discharges. Constraints on the electron heat diffusivity were derived from the steady-state electron energy equation by using the shape of the measured T_e profiles.

The results from these constraints were discussed and the expressions compared with empirical scaling relations. It is found that the χ_e scalings vary with the heating method and its specific dependence on the plasma parameters. There is a strong interaction between the heating, the electron thermal conduction and the electron temperature. The profiles of these quantities have to adjust self-consistently. With ohmic heating the stationary state reached is characterized by χ_e^{OH} and Gaussian-shaped $T_e(r)$, whereas with neutral injection χ_e^L and triangular T_e profiles are obtained. It is further concluded that in the intermediate range complex χ_e scalings result which cannot simply be represented by superposing the ohmic and L scalings.

Scanning the injection power and studying the L transport after neutral-beam heating showed that deviations from the ohmic scaling occur if P_b or P_{ie} locally exceed $0.3\,\eta j_t^2$. The transition to the L regime was shown to correlate with the ratio $P_b/(\eta j_t^2)$ in the confinement zone. Moreover, it is found that non-ohmic electron heating is required for the L confinement,

while direct ion heating and beam fuelling are not. The auxiliary heating is thought to perturb the stationary ohmic state with self-consistent profiles. The associated transition to a new state with different χ_e scaling and T_e profile shape suggests that a self-regulating or feedback process (connected with strong turbulence) is present. It apparently adjusts the χ_e scaling to the injection heating, whose variation with the plasma parameters differs from that of the ohmic heating. It was shown that with this feedback process the T_e profile shape is not constrained by the profile consistency. The transition between the OH and L regimes is smooth, i.e. there are no indications of threshold behaviour. At the smallest injection power applied, the plasma parameters are not markedly modified, so that a transition to other instabilities and/or saturation effects becomes very unlikely. This means that the change in χ_e scaling with neutral injection should not be due to a different transport mechanism.

Measurements of density fluctuations in ohmically and neutral-beam-heated plasmas show broad frequency spectra around the electron diamagnetic drift frequency. They suggest that the anomalous transport is connected with strong turbulence driven by drift instabilities. The saturated states of such highly turbulent plasmas and the corresponding scalings of the fluctuation level and electron heat diffusivity should no longer be sensitive to the type of a single instability. Many modes are expected to constitute something like a turbulent background medium. This model is compatible with the result that the same empirical χ_e^{OH} scaling is found in all collisionality regimes, where different modes are linearly unstable, e.g. dissipative (collisional) drift modes, universal (collisionless) drift modes and trapped-particle modes. Such highly turbulent states also support the above conclusion that the ohmic and L scalings are not due to different instabilities but rather result from the adjustment to the heating method by a self-regulating process.

References

/1/ Becker, G., ASDEX Team, Neutral Injection Team, Nucl. Fusion 22 (1982) 1589.

/2/ Becker, G., Campbell, D., Eberhagen, A., Gehre, O., Gernhardt, J., et al., Nucl. Fusion 23 (1983) 1293.

/3/ Becker, G., Nucl. Fusion 24 (1984) 1364.

/4/ Kaye, S.M., Goldston, R.J., Bell, M., Bol, K., Bitter, M., et al., Nucl. Fusion 24 (1984) 1303.

/5/ Post, D.E., Singer, C.E., McKenney, A.M., BALDUR: A One-dimensional Plasma Transport Code, PPPL Transport Group, TFTR Physics Group, Report 33 (1981).

/6/ Becker, G., ASDEX Team, Neutral Injection Team, Analysis of Local Transport in Neutral-beam-heated L and H Plasmas of ASDEX, Max-Planck-Institut für Plasmaphysik, Garching, Rep. IPP III/98 (1984).

/7/ Coppi, B., Comments Plasma Phys. Cont. Fusion 5 (1980) 261.

/8/ Wagner, F., Gruber, O., Bartiromo, R., Becker, G., Bosch, H.S., et al., Proc. 12th Europ. Conf. on Contr. Fusion and Plasma Physics, Budapest 1985, Vol. I, p. 335.

/9/ Coppi, B., Mazzucato, E., Phys. Lett. 71A (1979) 337.

Figure Captions

Fig. 1: $T_e(r,t)$ after the beginning of neutral injection (t_{on} = 1.12 s) measured by multi-pulse Thomson scattering in an L discharge with $\bar{n} = 2.4 \times 10^{13}$ cm^{-3}, I_p = 280 kA and P_{abs} = 2.0 MW. The shaded area denotes the confinement zone.

Fig. 2: Approximately homogeneous electron thermal diffusivity from simulations versus absorbed beam power ($\bar{n} = 2.5 \times 10^{13}$ cm^{-3}). For comparison, the ohmic χ_e (2a/3) value (cross) is shown.

Fig. 3: $\chi_e(r)$ in the confinement zone (shaded) with ohmic heating and neutral-beam heating with two sources.

Fig. 4: Ratio of the beam power density and ohmic power density versus radius from simulations of the power scan of Fig. 2.

Fig. 5: As in Fig. 1, but after the end of neutral injection (t_{off} = 1.52 s).

Fig. 6: Ratio of the power densities of ion-electron energy transfer and ohmic heating versus radius after the end of the injection period (t_{off} = 1.31 s).

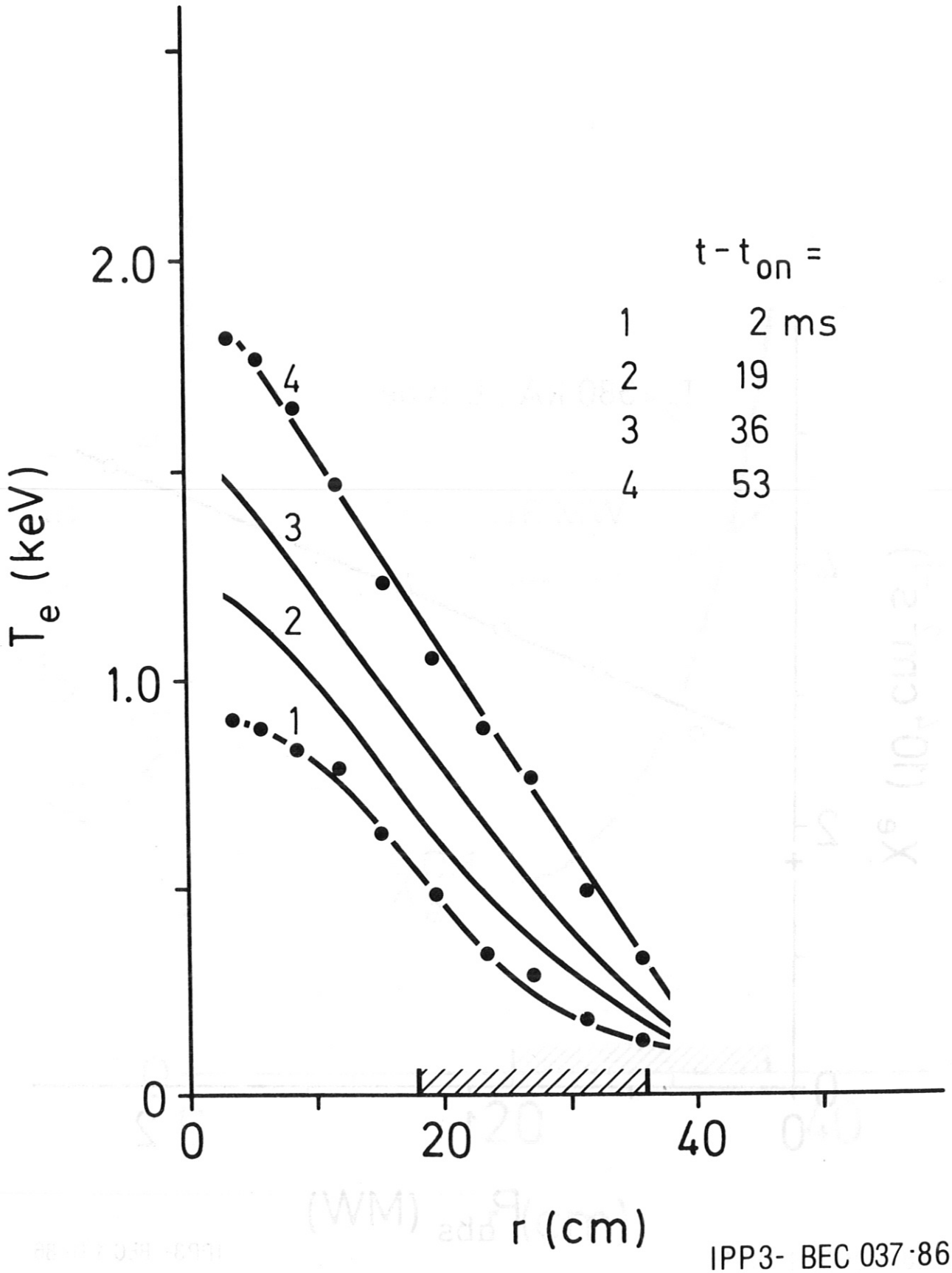

Fig. 1

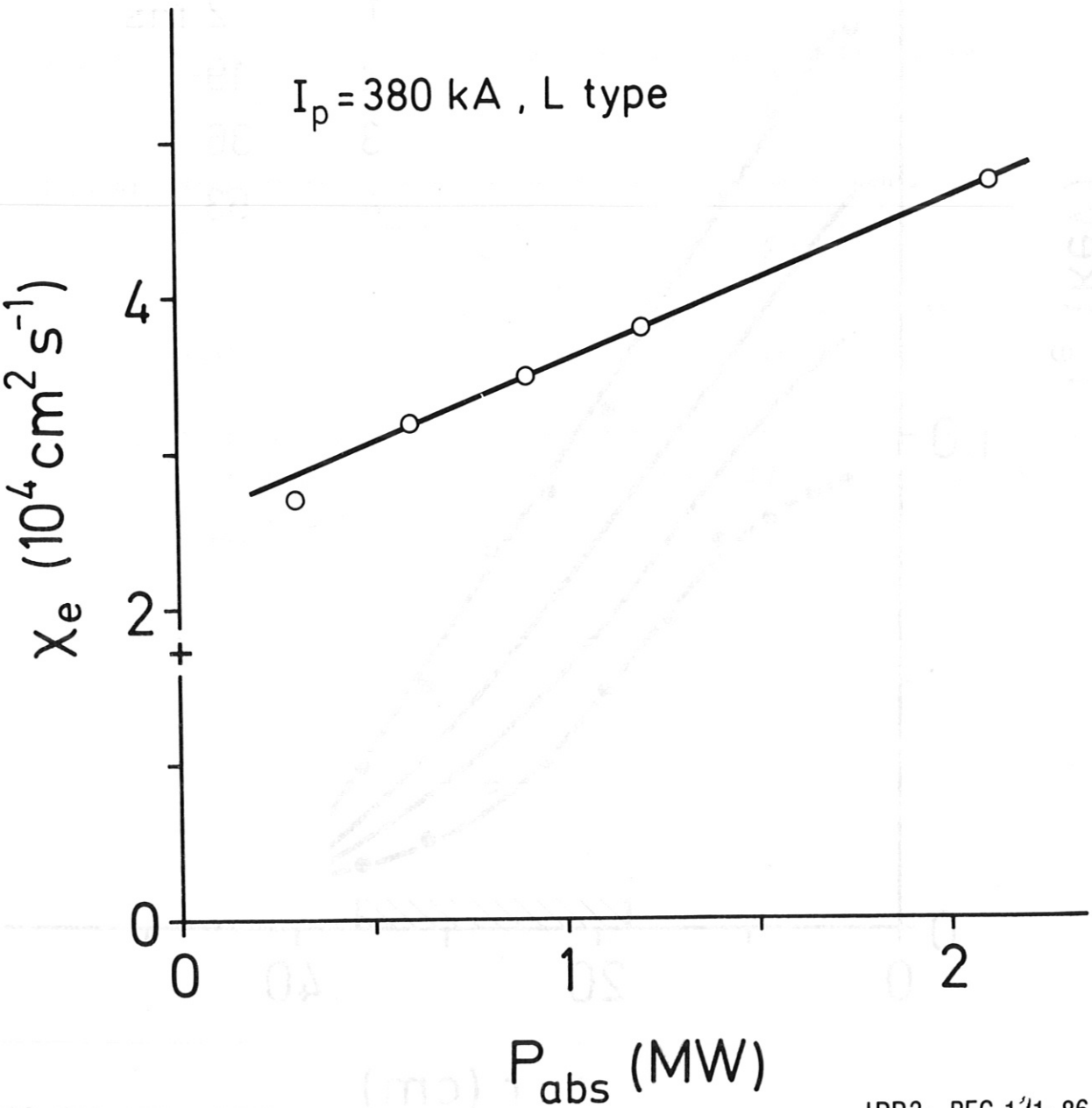

Fig. 2

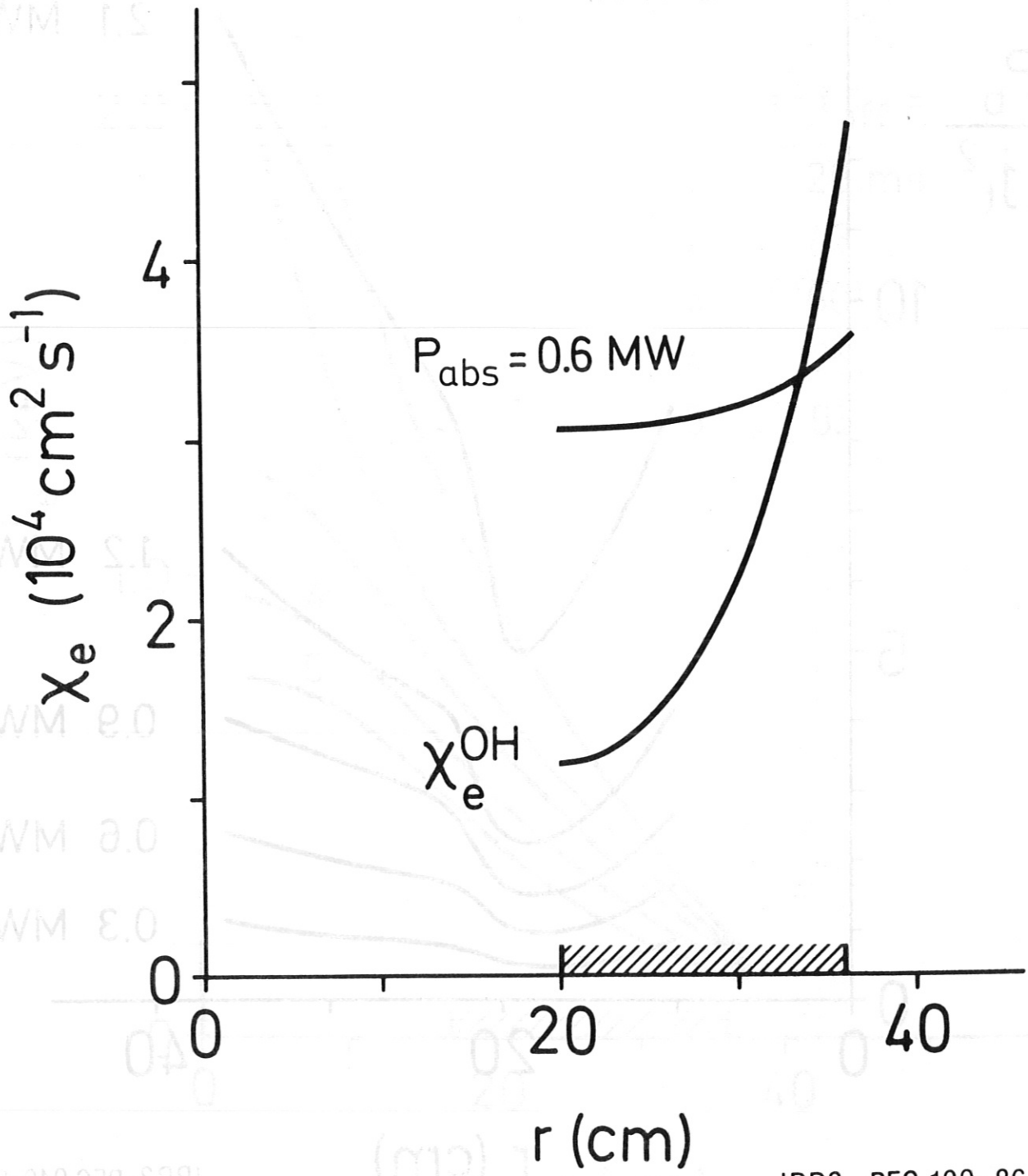

Fig. 3

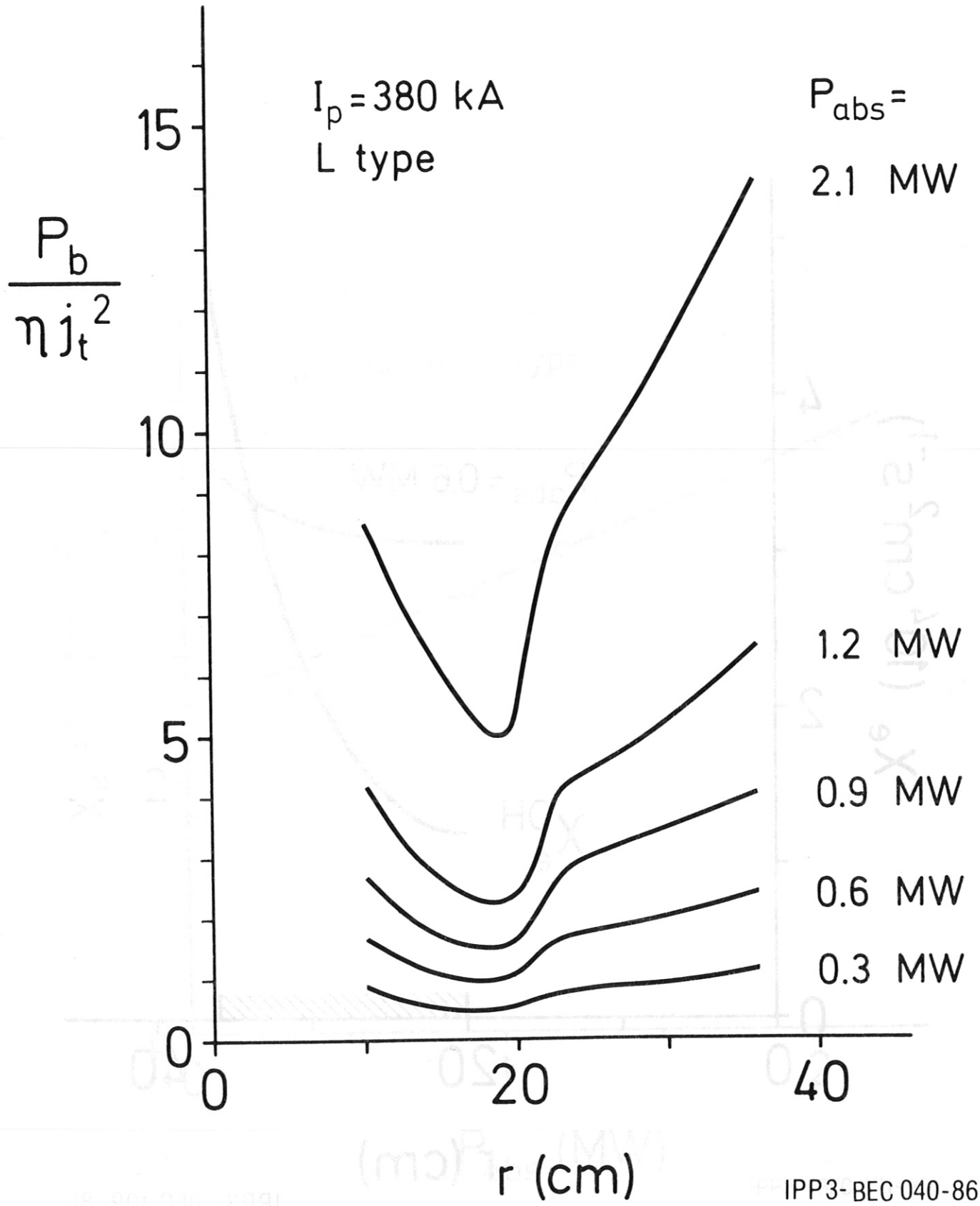
$I_p = 380$ kA
L type
P_{abs} =
2.1 MW
1.2 MW
0.9 MW
0.6 MW
0.3 MW
$\frac{P_b}{\eta j_t^2}$
15
10
5
0
0
20
40
r (cm)
IPP3-BEC 040-86

Fig. 4

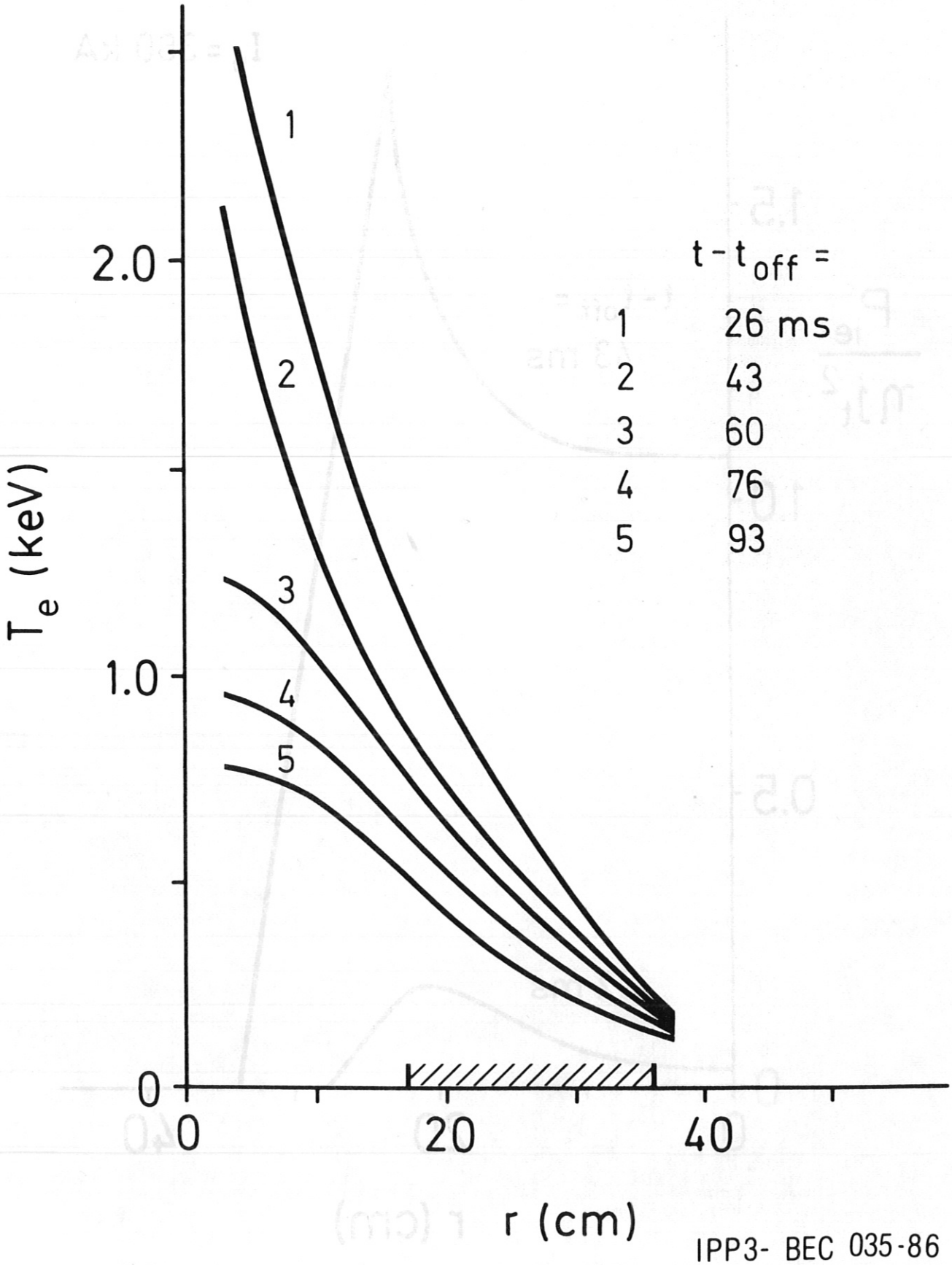
T_e (keV)
2.0
1.0
0
0
20
40
r (cm)
1
2
3
4
5
$t - t_{off}$ =
1 26 ms
2 43
3 60
4 76
5 93
IPP3- BEC 035-86

Fig. 5

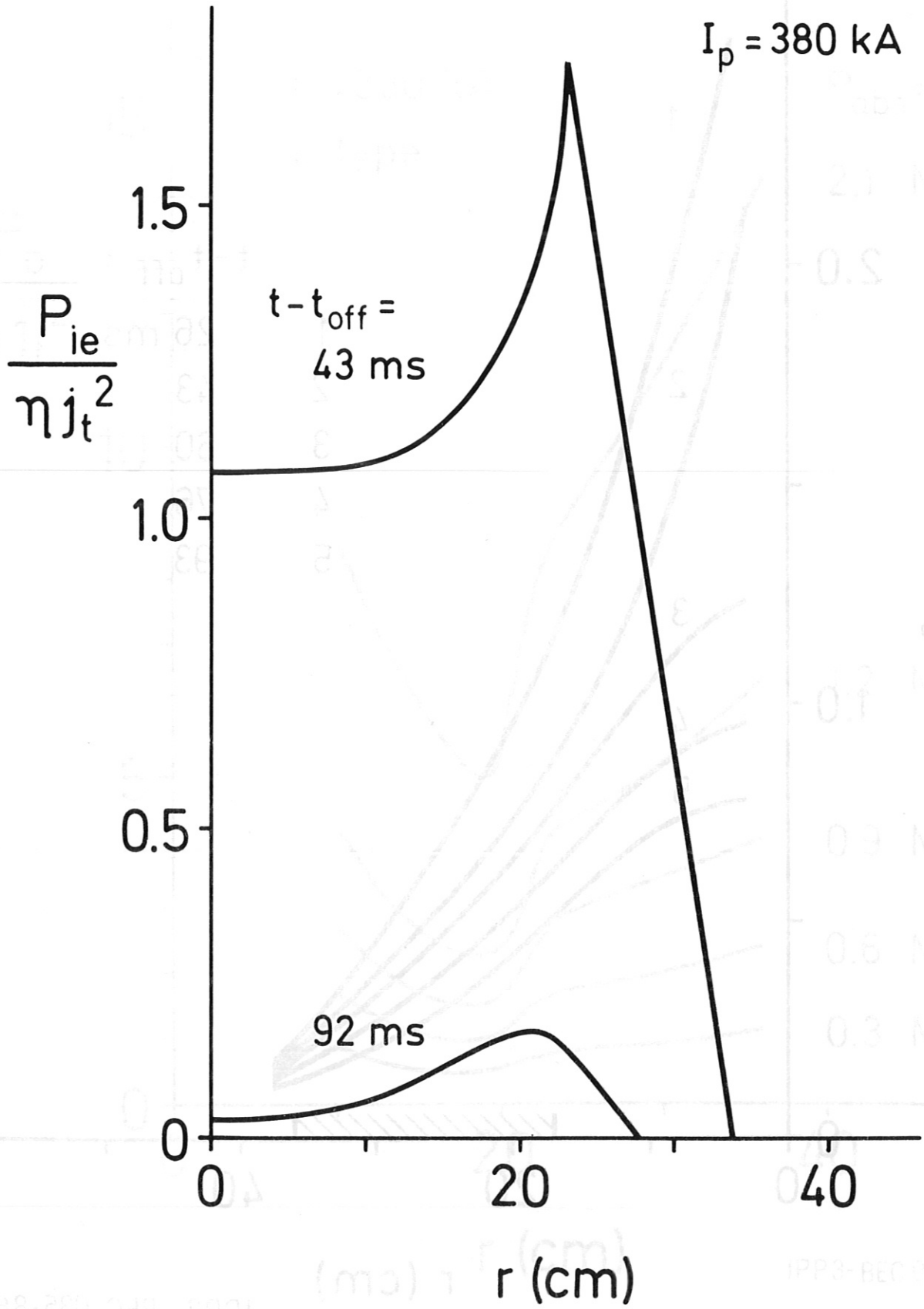

Fig. 6

IPP3- BEC 130-86